

Low-Energy $\bar{K}N$ and Pion-Hyperon Interactions. I. K -Matrix Analysis of K^-p Reactions*

B. R. MARTIN† AND M. SAKITT

Brookhaven National Laboratory, Upton, New York 11973

(Received 18 March 1969)

A nine-parameter K -matrix formalism for the low-energy K^-p interaction is described. These parameters are then determined by fitting the existing experimental data. A good fit is obtained to the data, and some properties of the solution are discussed.

1. INTRODUCTION

THE K^-p interaction is one of the few strange-particle scattering processes directly accessible to experiment. Consequently, much work has been devoted to its study. Unfortunately, the multichannel nature of the interaction, even at threshold, causes considerable complications in the analysis of the data. Early attempts at analyzing the low-energy data¹⁻³ involved expanding the $\bar{K}N$ amplitudes in powers of the center-of-mass momentum and kept only the first terms (i.e., the scattering lengths). This "constant scattering length" approach required six parameters for an adequate fit to all the K^-p data, as they existed at the time, below a kaon laboratory momentum $k_L \sim 300$ MeV/c, and strongly suggested that the $Y_0^*(1405)$ resonance was an s -wave virtual bound state of the $\bar{K}N$ system. The above approach, however, ignores important features of the multichannel nature of the problem, and uses scattering amplitudes with incorrect analytic properties. For example, the imaginary part of the $I=0$ elastic $\bar{K}N$ amplitude in the "constant scattering length" approach does not vanish at the $\pi\Sigma$ threshold, as it clearly should. Although this fact could conceivably be unimportant if the amplitude is used in the $\bar{K}N$ physical region, it is less likely to be unimportant in applications where the $\bar{K}N$ amplitude is used in the unphysical region between the $\pi\Sigma$ and $\bar{K}N$ thresholds.⁴

Unitary amplitudes with better analytic properties may be most simply constructed in a multichannel approach based on the use of the K matrix. Dalitz and Tuan⁵ first gave the necessary formalism for the case where the K -matrix elements are constants (we shall call this the "zero-range" approximation), and later

Shaw and Ross⁶ considered the case where effective range terms are included.

Recently, the method of Shaw and Ross⁶ has been used by Kim⁷ to analyze $\bar{K}N$ data in the momentum range $k_L < 550$ MeV/c. Kim includes s , p , and d waves and uses 44 parameters in the resulting fit. However, since neither the p -wave nor the d -wave parameters can be uniquely determined from the fit, the role of the 30 parameters describing these waves is not entirely clear. In this situation, a fruitful question to examine is the nature of the s -wave interaction deduced solely from the K^-p data below 300 MeV/c, i.e., from that region known experimentally to be dominated by s waves, and for which the production of three-particle states is negligible. This is the problem which we will examine in this paper. We will work with a K -matrix formulation in the zero-range approximation, and determine from the existing experimental data the nine parameters which are necessary in such a description. In the following paper, several applications of the resulting K -matrix parameters will be discussed.

Section 2 contains an outline of the K -matrix approach in the zero-range approximation. A brief discussion of the analyzed data is given in Sec. 3, followed in Sec. 4 by the results of the analysis. Finally, Sec. 5 contains a summary of results.

2. K -MATRIX FORMULATION

The K -matrix description of low-energy reactions $\bar{K}N$ has been given by Dalitz and Tuan,⁵ whose method will follow here. For exactness we give below those formulas which we will need for the analysis.

The K matrix is defined in terms of the usual T matrix by

$$T - iKFT = K, \quad (1)$$

where \mathbf{F} is a matrix of phase-space densities. Time-reversal invariance and Hermiticity ensure that the elements of K are real and that K is symmetric. Thus for the two-channel $\bar{K}N/\pi\Sigma$ problem in the $I=0$ state,

* Work performed under the auspices of the U. S. Atomic Energy Commission.

† Present address: Department of Physics, University College, London, England

¹ W. E. Humphrey and R. R. Ross, Phys. Rev. **127**, 1305 (1962).

² M. Sakitt, T. B. Day, R. G. Glasser, N. Seeman, J. Friedman, W. E. Humphrey, and R. R. Ross, Phys. Rev. **139**, B719 (1965).

³ J. K. Kim, Phys. Rev. Letters **14**, 29 (1965).

⁴ This is the case, for example, in applications involving kaon-nucleon dispersion relations. An example involving the use of kaon-nucleon forward dispersion relations is given in B. R. Martin and M. Sakitt, following paper, Phys. Rev. **183**, 1352 (1969).

⁵ R. H. Dalitz and S. F. Tuan, Ann. Phys. (N. Y.) **10**, 307 (1960).

⁶ G. L. Shaw and M. Ross, Phys. Rev. **126**, 814 (1962).

⁷ J. K. Kim, Phys. Rev. Letters **19**, 1074 (1967).

we may write

$$\mathbf{K}^0 = \begin{pmatrix} \alpha_0 & \beta_0 \\ \beta_0 & \gamma_0 \end{pmatrix} \begin{matrix} \bar{K}N \\ \pi\Sigma \end{matrix}, \quad (2)$$

$$\begin{matrix} \bar{K}N \\ \pi\Sigma \end{matrix}$$

where, in the zero-range approximation, α_0 , β_0 , and γ_0 are constants. Using Eq. (2) in (1), and solving for the elastic $\bar{K}N$ amplitude, gives

$$k \cot \delta_0^K = 1/A_0 \quad (3)$$

for the $I=0$ $\bar{K}N$ phase shift, where

$$\text{Re}A_0 \equiv a_0 = \alpha_0 - \frac{k_\Sigma^2 \gamma_0 \beta_0^2}{1 + (k_\Sigma \gamma_0)^2} \quad (4)$$

$$\text{Im}A_0 \equiv b_0 = \frac{k_\Sigma \beta_0^2}{1 + (k_\Sigma \gamma_0)^2}, \quad (5)$$

and k (k_Σ) denotes the center-of-mass three-momentum in the $\bar{K}N$ ($\pi\Sigma$) elastic channel. The "constant scattering length" approach is to set $A_0 = \text{const}$, but, as remarked in the Introduction, this is clearly incompatible with the analytic properties implied by Eq. (5). The amplitude for the production process $\bar{K}N \rightarrow \pi\Sigma$ and the elastic amplitude for $\pi\Sigma \rightarrow \pi\Sigma$ may be found in a similar manner.

For the $I=1$ state there are two hyperon channels, $\pi\Lambda$ and $\pi\Sigma$, and hence we have a three-channel problem. We shall define the $I=1$ K matrix by

$$\mathbf{K}^1 = \begin{pmatrix} \alpha_1 & \beta_\Sigma & \beta_\Lambda \\ \beta_\Sigma & \gamma_{\Sigma\Sigma} & \gamma_{\Sigma\Lambda} \\ \beta_\Lambda & \gamma_{\Sigma\Lambda} & \gamma_{\Lambda\Lambda} \end{pmatrix} \begin{matrix} \bar{K}N \\ \pi\Sigma \\ \pi\Lambda \end{matrix}, \quad (6)$$

$$\begin{matrix} \bar{K}N \\ \pi\Sigma \\ \pi\Lambda \end{matrix}$$

where all the parameters are constants, and we shall denote by k_Λ the center-of-mass three-momentum of the $\pi\Lambda$ final state. Then, proceeding as for the $I=0$ states, the following results may be derived for δ_1^K , the $I=1$ s -wave $\bar{K}N$ phase shift:

$$k \cot \delta_1^K = 1/A_1, \quad (7)$$

where

$$\text{Re}A_1 \equiv a_1 = \alpha_1 + \frac{\theta_1 \theta_3 + \theta_2 \theta_4}{\theta_3^2 + \theta_4^2}, \quad (8)$$

$$\text{Im}A_1 \equiv b_1 = \frac{\theta_2 \theta_3 - \theta_1 \theta_4}{\theta_3^2 + \theta_4^2} \quad (9)$$

and

$$\theta_1 = k_\Lambda k_\Sigma (\beta_\Lambda^2 \gamma_{\Sigma\Sigma} - 2\beta_\Lambda \beta_\Sigma \gamma_{\Sigma\Lambda} + \beta_\Sigma^2 \gamma_{\Lambda\Lambda}), \quad (10)$$

$$\theta_2 = \beta_\Lambda^2 k_\Lambda + \beta_\Sigma^2 k_\Sigma, \quad (11)$$

$$\theta_3 = 1 - k_\Lambda k_\Sigma (\gamma_{\Lambda\Lambda} \gamma_{\Sigma\Sigma} - \gamma_{\Sigma\Lambda}^2), \quad (12)$$

$$\theta_4 = - (k_\Lambda \gamma_{\Lambda\Lambda} + k_\Sigma \gamma_{\Sigma\Sigma}). \quad (13)$$

As for the $I=0$ case, the hyperon production amplitudes and pion-hyperon scattering amplitudes may be found by similar means.

Because, in practice, one fits cross sections for definite charge states, it is convenient to define two further quantities given in terms of the K -matrix parameters. One of these is $\Phi \equiv \Phi_0 - \Phi_1$, where Φ_0 and Φ_1 are the phases of the $\pi\Sigma$ production amplitudes, in a state for which $I=0$ and 1, respectively. The other quantity is the ratio of the cross section for $\pi\Lambda$ production to that for the total hyperon production in an $I=1$ state, i.e.,

$$\epsilon = \frac{\sigma(\pi\Lambda)}{[\sigma(\pi\Sigma) + \sigma(\pi\Lambda)]_{I=1}}. \quad (14)$$

In terms of Φ and ϵ , the cross sections for the production of specific charge states from an initial K^-p state are

$$\sigma(\pi^+\Sigma^-) = \frac{1}{6}\sigma_0 + \frac{1}{4}(1-\epsilon)\sigma_1 + \left[\frac{1}{6}\sigma_0\sigma_1(1-\epsilon)\right]^{1/2} \cos\Phi, \quad (15)$$

$$\sigma(\pi^-\Sigma^+) = \frac{1}{6}\sigma_0 + \frac{1}{4}(1-\epsilon)\sigma_1 - \left[\frac{1}{6}\sigma_0\sigma_1(1-\epsilon)\right]^{1/2} \cos\Phi, \quad (16)$$

$$\sigma(\pi^0\Sigma^0) = \frac{1}{6}\sigma_0, \quad (17)$$

$$\sigma(\pi^0\Lambda^0) = \frac{1}{2}\sigma_1\epsilon, \quad (18)$$

where σ_I ($I=0, 1$) is the total hyperon production cross section in an isospin state I .

The charge independence implicitly assumed in the above discussion is violated in two distinct ways. First, the masses of the particles in a given isospin multiplet will no longer be equal. This can give quite appreciable effects at very low momentum and means, in particular, that the charge-exchange process $K^-p \rightarrow \bar{K}^0n$ must be treated explicitly. These effects can be incorporated in a simple manner by using the physical masses of the particles. Secondly, the elements of the K matrix will themselves be modified. We will include only those modifications due to the Coulomb interaction, since other effects are expected to be much smaller. The inclusion of Coulomb effects has been extensively discussed by Dalitz and Tuan,⁵ and we will merely quote their results, but first it is necessary to define a few subsidiary quantities.

If $B = \hbar^2/M_\pi e^2$ denotes the Bohr radius of the initial K^-p system, then we shall define a Coulomb correction factor

$$C = (2\pi/kB)(1 - e^{-2\pi/kB})^{-1}. \quad (19)$$

Furthermore, if we set $k_c = kC$ and denote the center-of-mass three-momentum in the \bar{K}^0n channel by k_0 , then we shall define

$$D = (1 - iXk_0)[1 - iXk_c(1 - i\lambda)] + k_0k_c(1 - i\lambda)Y^2, \quad (20)$$

where

$$X = \frac{1}{2}(A_1 + A_0), \quad Y = \frac{1}{2}(A_1 - A_0), \quad (21)$$

and λ is a complicated function of the interaction radius given in Ref. 5. In terms of the above quantities the cross sections, modified by Coulomb effects, are:

(1) elastic K^-p differential cross section

$$\frac{d\sigma_{el}(\theta)}{d\Omega} = \left| \frac{\csc^2(\frac{1}{2}\theta)}{2Bk^2} \exp\left(\frac{2i}{k} \ln[\sin(\frac{1}{2}\theta)]\right) + \frac{C}{2D} (A_0 + A_1 - 2ik_0 A_0 A_1) \right|^2, \quad (22)$$

(2) charge-exchange cross section

$$\sigma_{ch. ex.} = \pi C \frac{k_0}{k} \left| \frac{A_1 - A_0}{D} \right|^2, \quad (23)$$

(3) total hyperon production cross sections for states with $I=0, 1$

$$\sigma_0 = 4\pi C \frac{\text{Im}A_0}{k} \left| \frac{1 - ik_0 A_1}{D} \right|^2, \quad (24)$$

$$\sigma_1 = 4\pi C \frac{\text{Im}A_1}{k} \left| \frac{1 - ik_0 A_0}{D} \right|^2. \quad (25)$$

Cross sections for hyperon production in given charge states may then be found from Eqs. (15)–(18). The results are insensitive to any interaction radius $\lesssim 1$ F.

3. EXPERIMENTAL SITUATION

We will now briefly review the existing experimental data that are appropriate to determine the nine K -matrix parameters. One of the earliest studies attempted was by Humphrey and Ross¹ in 1962. Using a hydrogen bubble chamber exposed to a stopping K^- -meson beam, they studied the following reactions:

- (a) $K^- + p \rightarrow K^- + p$
- (b) $\quad \quad \rightarrow \bar{K}^0 + n$
- (c) $\quad \quad \rightarrow \Sigma^\pm + \pi^\mp$
- (d) $\quad \quad \rightarrow \Sigma^0 + \pi^0$
- (e) $\quad \quad \rightarrow \Lambda^0 + \pi^0$,

and, using a six-parameter "constant scattering length" formalism, determined two possible solutions. Their favored solution neither fitted onto the higher-energy data⁸ nor yielded a bound state which would correspond to the $Y_0^*(1405)$. In order to resolve these discrepancies, two experiments with significantly higher statistics were performed by Kim³ and by Sakitt *et al.*² Using the same formalism as in the earlier study, each experiment obtained a solution which agreed with the higher-energy data and predicted the $Y_0^*(1405)$ as a $\bar{K}N$ s -wave bound state. Kim examined reactions (a)–(e) and used the older Humphrey-Ross $(\Sigma^+ + \Sigma^-)/(\Sigma^0 + \Lambda)$ branching ratio in his analysis. Sakitt *et al.* examined reactions (a) and (c) and used the older Humphrey-Ross at-rest

branching ratios and charge-exchange data. Both experiments found isotropic distributions in the center-of-mass scattering angle, for the various channels studies, which justified the use of an s -wave formalism. After these analyses, new data, with better statistics, were published for the charge-exchange channel.^{9,10}

Since all of the newer data^{2,3,9,10} gave consistent results using the constant scattering length formalism, and since they are statistically more significant than the older data,¹ we use the newer data to determine the nine parameters in our formalism. The only exception to this is the at-rest branching ratios, some of which have not been improved from the earlier Humphrey-Ross results¹; we therefore do use these earlier at-rest branching ratios. It is interesting to note that all the data that we have mentioned come from experiments using bubble chambers, and therefore the experiments have similar problems and limitations. The bulk of the events that are observed result from a K meson having stopped in the bubble chamber and having been captured by the proton from an orbital s state. In the hyperon production reactions (c)–(e) it is not possible to separate clearly at-rest events from in-flight events below a K^- laboratory momentum of about 80 MeV/c. For the elastic scattering event it is necessary to have a lower limit on the K^- laboratory momentum of about 100 MeV/c to ensure reasonable lengths for the recoil particles. It is believed that the scanning efficiencies, which obviously depend on the recoil lengths, would be unreliable below this limit.

The data used in our analysis are shown in Figs. 1–6. While Fig. 1 shows the elastic cross section after integrating over the center-of-mass scattering angle, we have used the data for our estimation of the K -matrix parameters only after dividing them into various angular intervals, as was done by the original authors.^{2,3} The use of the differential cross section makes maximum use of Coulomb nuclear interference information.

4. DETERMINATION OF K -MATRIX PARAMETERS

Using the formalism described in Sec. 2, we calculate, as a function of the nine parameters, theoretical values for all the experimentally observed quantities. We define a χ^2 function

$$\chi^2(\alpha_0, \gamma_0, \beta_0, \alpha_1, \beta_1, \beta_2, \gamma_{\Sigma\Sigma}, \gamma_{\Lambda\Lambda}, \gamma_{\Sigma\Lambda}) = \sum_{a,j,k} (\sigma_{aj}^T - \sigma_{aj}^M) (V^a)^{-1}_{jk} (\sigma_{ak}^T - \sigma_{ak}^M),$$

where V^a is the variance matrix for the experimental results of type a , σ_{aj}^T is the theoretical cross section of type a for the momentum bin j , and σ_{aj}^M is the measured cross section of type a for the momentum bin j . The

⁸ M. B. Watson, M. Ferro-Luzzi, and R. D. Tripp, Phys. Rev. **131**, 2248 (1963).

⁹ G. S. Abrams and B. Sechi-Zorn, Phys. Rev. **139**, B454 (1965).

¹⁰ W. Kittel, G. Otter, and I. Wacek, Phys. Letters **21**, 349 (1966).

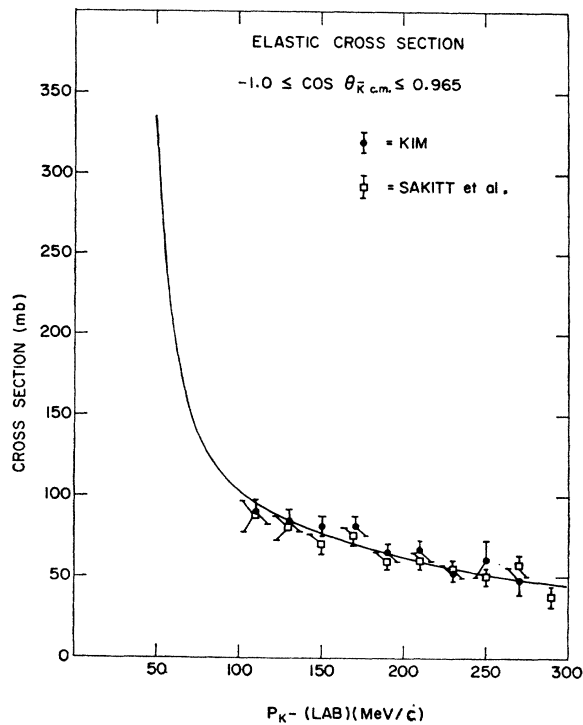


FIG. 1. Cross section for $K^- + p \rightarrow K^- + p$. The solid curve is the theoretical solution. Experimental points are from Sakitt *et al.* (Ref. 2) and Kim (Ref. 3).

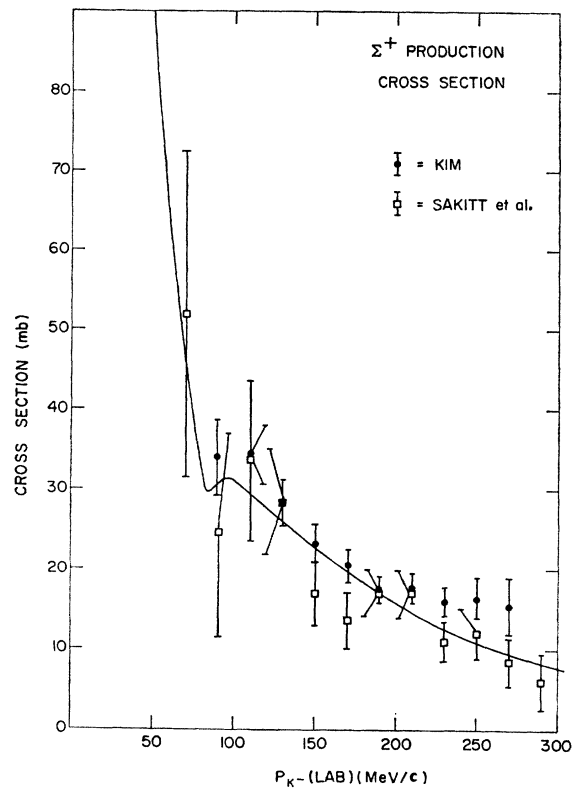


FIG. 3. Cross section for $K^- + p \rightarrow \Sigma^+ + \pi^-$. The solid curve is the theoretical solution. Experimental points are from Sakitt *et al.* (Ref. 2) and Kim (Ref. 3).

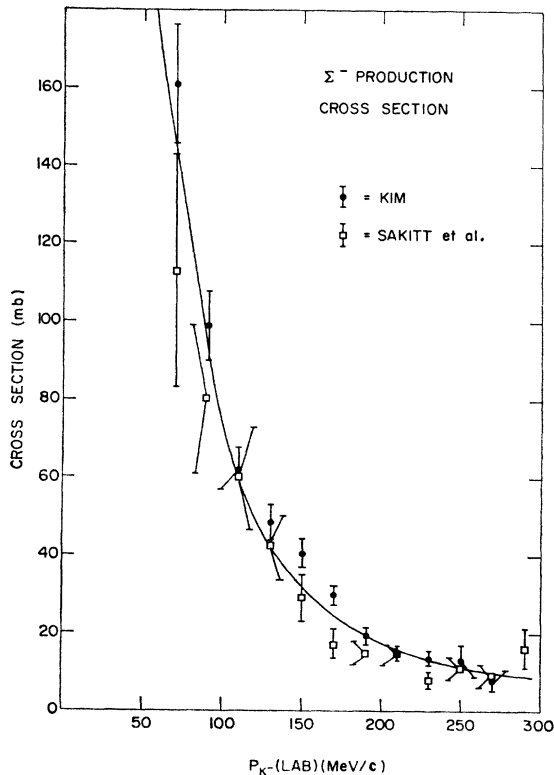


FIG. 2. Cross section for $K^- + p \rightarrow \Sigma^- + \pi^+$. The solid curve is the theoretical solution. Experimental points are from Sakitt *et al.* (Ref. 2) and Kim (Ref. 3).

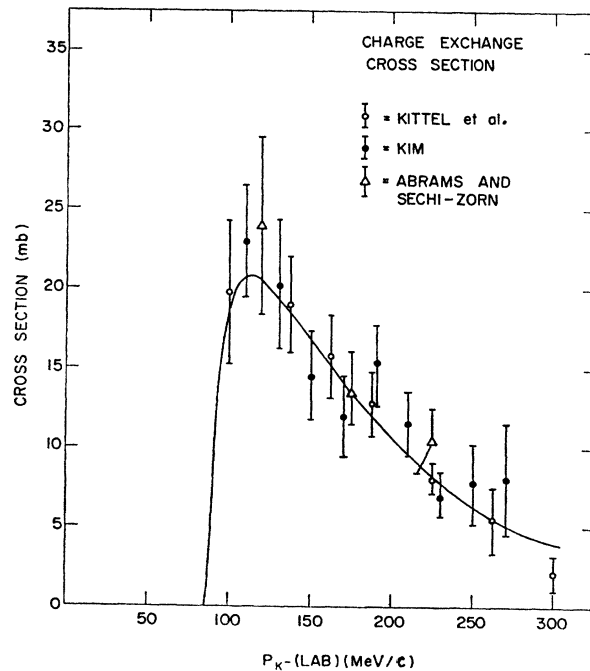


FIG. 4. Cross section for $K^- + p \rightarrow \bar{K}^0 + n$. The solid curve is the theoretical solution. Experimental points are from Kim (Ref. 3), Abrams *et al.* (Ref. 9), and Kittel *et al.* (Ref. 10).

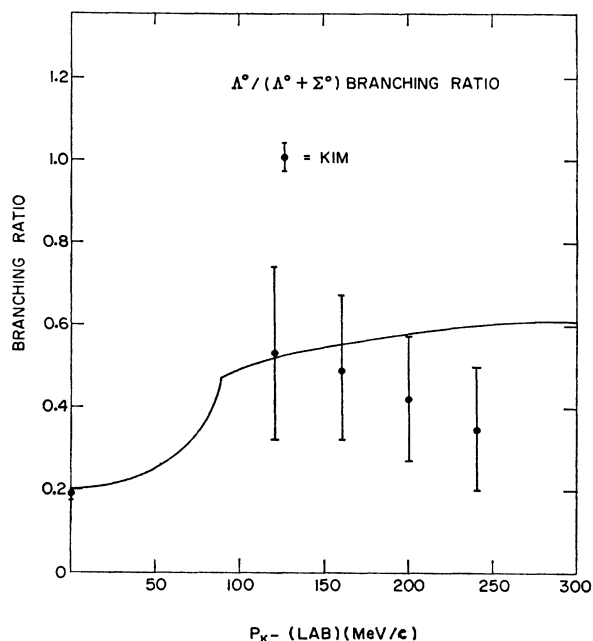


FIG. 5. Branching ratio for $\Lambda\pi^0/(\Lambda\pi^0+\Sigma^0\pi^0)$. The solid curve is the theoretical solution. Experimental points are from Kim (Ref. 3).

set of parameters which yields a minimum in χ^2 is defined as our best estimate of the K -matrix parameters, and the value of χ^2 at that minimum gives us a con-

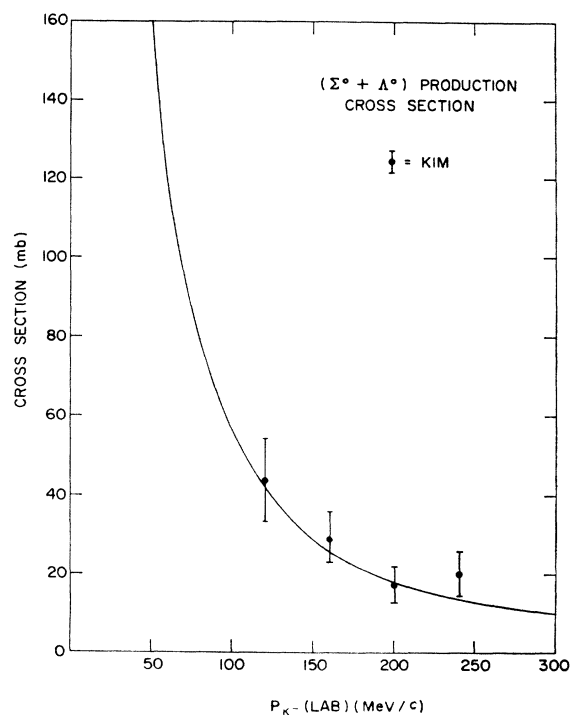


FIG. 6. Cross section for $K^-p \rightarrow (\Sigma^0 \text{ or } \Lambda^0) + \pi^0$. The solid curve is the theoretical solution. Experimental points are from Kim (Ref. 3).

fidence level for the fit. In addition, the shape of χ^2 in the region of the minimum gives us an estimate of the error for the determined parameters.

In order to find a minimum in this nine-dimensional space, we used a program called MINFUN.¹¹ Given initial values for the parameters, this program will evaluate the nine-dimensional gradient in an iterative manner, and, by moving the parameters in the necessary direction, will find a minimum. Having found a minimum, it will calculate an error matrix for the parameters, assuming that the region in the local vicinity of the minimum can be adequately described by a quadratic expansion in the parameter variables.

A summary of the data and their individual contributions to the over-all χ^2 is shown in Table I. The χ^2 minimum found yielded the following estimates for the nine K -matrix parameters in fermis:

$$\begin{aligned} \alpha_0 &= -1.879, & \beta_0 &= -0.919, & \gamma_0 &= -0.356; \\ \alpha_1 &= 0.222, & \beta_2 &= 0.781, & \beta_\Lambda &= 0.381; \\ \gamma_{\Sigma\Sigma} &= 0.919, & \gamma_{\Sigma\Lambda} &= -0.174, & \gamma_{\Lambda\Lambda} &= 0.463. \end{aligned}$$

The variance matrix for our solution is shown in Table II. It is clear from that matrix that several of the parameters are highly correlated, and that using merely the diagonal errors as standard deviations for the propagation of errors can be quite misleading. The χ^2 value at the minimum is 186. Since we have 179 measurements from which we determine nine parameters, we have 170 degrees of freedom. We therefore have a confidence level of 19% for our solution. This solution was found when we used starting values based on the solutions of Sakitt *et al.*² or of Kim.³ In addition, we made numerous searches after varying the values of the initial parameters in arbitrary directions, and we always obtained the original minimum. We believe that, though perhaps not extremely well determined, our solution is unique in the context of this formalism.

The agreement between experiment and theory is shown in a qualitative manner in Figs. 1-6. Over the data we have drawn the theoretical cross section determined from our solutions. Table III contains calculated values for the $I=0$ and $I=1$ Σ -production cross sections and the relative phase between the two production amplitudes, all as a function of K^- laboratory momentum.

5. CONCLUSIONS

Using a zero-range approximation, where the K -matrix elements are constant, we have adequately described the existing data on low-energy K^-p interactions. This formalism avoids the incorrect analytic

¹¹ W. E. Humphrey and A. H. Rosenfeld, *Ann. Rev. Nucl. Sci.* **13**, 103 (1963).

TABLE I. Measurements used in the determination of the K -matrix parameters.

Measured quantity	No. of measurements	Range of K^- lab momentum (MeV/c)	χ^2 contribution	Ref.
$\int_{-1.0}^{0.85} \frac{d\sigma_{e1}}{d\Omega}$	10	100-300	22.7	2
$\int_{0.85}^{0.90} \frac{d\sigma_{e1}}{d\Omega}$	10	100-300	5.3	2
$\int_{0.90}^{0.95} \frac{d\sigma_{e1}}{d\Omega}$	10	100-300	19.7	2
$\int_{0.95}^{0.966} \frac{d\sigma_{e1}}{d\Omega}$	10	100-300	13.4	2
$\int_{-0.965}^{0.60} \frac{d\sigma_{e1}}{d\Omega}$	9	100-280	11.2	3
$\int_{0.60}^{0.70} \frac{d\sigma_{e1}}{d\Omega}$	9	100-280	7.4	3
$\int_{0.70}^{0.80} \frac{d\sigma_{e1}}{d\Omega}$	9	100-280	5.0	3
$\int_{0.80}^{0.85} \frac{d\sigma_{e1}}{d\Omega}$	9	100-280	5.2	3
$\int_{0.85}^{0.90} \frac{d\sigma_{e1}}{d\Omega}$	9	100-280	3.9	3
$\int_{0.90}^{0.95} \frac{d\sigma_{e1}}{d\Omega}$	9	100-280	4.9	3
$\int_{0.95}^{0.965} \frac{d\sigma_{e1}}{d\Omega}$	9	100-280	3.8	3
$\sigma(K^- + p \rightarrow \bar{K}^0 + n)$	3	100-250	1.7	9
$\sigma(K^- + p \rightarrow \bar{K}^0 + n)$	9	100-280	7.2	3
$\sigma(K^- + p \rightarrow \bar{K}^0 + n)$	7	100-275	4.3	10
$\sigma(K^- + p \rightarrow \Sigma^+ + \pi^-)$	12	60-300	7.2	2
$\sigma(K^- + p \rightarrow \Sigma^+ + \pi^-)$	10	80-280	14.2	3
$\sigma(K^- + p \rightarrow \Sigma^- + \pi^+)$	12	60-300	21.1	2
$\sigma(K^- + p \rightarrow \Sigma^- + \pi^+)$	11	60-280	20.4	3
$\Gamma(K^- + p \rightarrow \Sigma^- + \pi^+)$	1	at rest	0.3	1
$\Gamma(K^- + p \rightarrow \Sigma^+ + \pi^-)$				
$\Gamma(K^- + p \rightarrow \Sigma^- + \pi^+)$	1	at rest	0.1	3
$\Gamma(K^- + p \rightarrow \Sigma^+ + \pi^-)$				
$\sigma(K^- + p \rightarrow \Lambda + \pi^0) + \sigma(K^- + p \rightarrow \Sigma^0 + \pi^0)$	4	100-220	2.1	3
$\sigma(K^- + p \rightarrow \Lambda + \pi^0)$				
$\sigma(K^- + p \rightarrow \Lambda + \pi^0) + \sigma(K^- + p \rightarrow \Sigma^0 + \pi^0)$	4	100-260	3.7	3
$\Gamma(K^- + p \rightarrow \Sigma^+ + \pi^-) + \Gamma(K^- + p \rightarrow \Sigma^- + \pi^+)$	1	at rest	6.8	1
$\Gamma(K^- + p \rightarrow \Lambda + \pi^0) + \Gamma(K^- + p \rightarrow \Sigma^0 + \pi^0)$				
$\Gamma(K^- + p \rightarrow \Lambda + \pi^0)$	1	at rest	0.0	3
$\Gamma(K^- + p \rightarrow \Lambda + \pi^0) + \Gamma(K^- + p \rightarrow \Sigma^0 + \pi^0)$				
Total	179		185.6	

TABLE II. Variance matrix for the K -matrix solution. (Symmetric elements have not been duplicated.)

	α_0	β_0	γ_0	α_1	β_Σ	β_Δ	$\gamma_{\Sigma\Sigma}$	$\gamma_{\Sigma\Delta}$	$\gamma_{\Delta\Delta}$
α_0	4.91×10^{-4}								
β_0	-2.30×10^{-4}	1.65×10^{-4}							
γ_0	3.47×10^{-4}	-1.76×10^{-4}	2.93×10^{-4}						
α_1	3.77×10^{-4}	-1.47×10^{-4}	3.15×10^{-4}	4.81×10^{-4}					
β_Σ	9.43×10^{-5}	-1.61×10^{-5}	5.95×10^{-5}	5.13×10^{-5}	1.32×10^{-4}				
β_Δ	1.49×10^{-4}	-7.97×10^{-5}	1.35×10^{-4}	2.06×10^{-4}	-6.43×10^{-5}	1.57×10^{-4}			
$\gamma_{\Sigma\Sigma}$	6.02×10^{-5}	5.98×10^{-6}	1.95×10^{-5}	1.45×10^{-6}	1.56×10^{-4}	-1.09×10^{-4}	2.78×10^{-4}		
$\gamma_{\Sigma\Delta}$	2.10×10^{-4}	-1.31×10^{-4}	1.90×10^{-4}	2.08×10^{-4}	-5.54×10^{-5}	1.60×10^{-4}	-1.65×10^{-4}	2.40×10^{-4}	
$\gamma_{\Delta\Delta}$	1.89×10^{-5}	-8.20×10^{-6}	-7.11×10^{-6}	3.51×10^{-4}	-2.89×10^{-4}	3.5×10^{-4}	9.67×10^{-5}	-1.09×10^{-4}	4.99×10^{-5}

properties in the scattering amplitudes of the previous constant scattering length analyses^{1-3,9,10} which could be important in the application of these amplitudes to

TABLE III. Theoretical values for the Σ -production cross sections in the $I=0$ and 1 isotopic spin channel and the relative phase Φ between the two amplitudes.

K^- lab momentum (MeV/c)	σ_0 (mb)	σ_1 (mb)	Φ (rad)
50	720	222	-1.05
75	356	158	-0.98
100	173	146	-1.15
125	115	110	-1.30
150	81.3	85.8	-1.39
175	60.4	69.2	-1.46
200	46.5	57.2	-1.52
225	36.8	48.1	-1.57
250	29.8	40.9	-1.60
275	24.7	35.3	-1.63
300	20.8	30.7	-1.66

kaon-nucleon forward dispersion relations. By restricting the analysis to the low-energy region where the s -wave contributions completely dominate, we have avoided the complication of trying to include p and d waves, with the resulting large increase in parameters, as was done in a previous effective range analysis.⁷ In addition, unlike previous analyses, we have used all of the available reliable data rather than a particular subset of the total data. Including all of the data allows us to present a complete current description of the low-energy region of the K^-p system.

In the following paper we will discuss several applications of our solutions.

ACKNOWLEDGMENT

One of us (M.S.) would like to thank Dr. N. P. Samios for both his encouragement and support.